11th Australasian Fluid Mechanics Conference
University of Tasmania, Hobart, Australia
14-18 December 1992

NOVEL BUBBLES IN SALTY WATER

Michael BORGAS and Mark HIBBERD

CSIRO Division of Atmospheric Research
Private Bag 1, Mordialloc, VIC 3195
AUSTRALIA

ABSTRACT

Unusual bubbles have been observed when very salty water drips into a tank of stably stratified salty water. The bubbles, which are really thin spherical shells of air enclosing one of the impinging drops, and therefore complement the more common soap bubbles in air (Boys, 1890), descend until an equilibrium depth is reached where the net buoyancy vanishes. The thin air film, however, continues to drain and becomes ever thinner at its lowest point, while thickening at its apex. This process is relatively slow and the bubble appears stable and very nearly spherical for an extended period. Eventually, the film ruptures and a series of conventional air bubbles rise to the surface.

INTRODUCTION

The bubbles described in the abstract were the inadvertent outcome of cleaning a tank in which the convective boundary layer (CBL) is routinely simulated (Hibberd & Sawford, 1989). The tank is $80cm$ deep with plan area of approximately $5m^2$. After routine use, it is brimfull with salt water: the top 20 to $40cm$ is well mixed, but below this and to the bottom the salt water is stably stratified with linear density variation with depth ($\sim 0.001\ gcm^{-4}$). Above the water surface, at a height of several centimetres (this is a critical parameter for the formation of these bubbles), there is a porous membrane ($6mm$ thick sintered polyethelyne, $20\mu m$ pore size) covering the horizontal expanse of the tank. This membrane provides a mass flux of very salty water during a CBL run, but it is then flush with the water. After a run the membrane is raised slightly and cleaned. Detergent (Hoechst Arkopal N100) is added to aid the wetting of the pores and the upper surface of the membrane is covered with fresh water which percolates through (collecting residual salt *and* detergent), dripping onto the well-mixed layer at random horizontal positions and random instants in time. Depending on the height, the detergent, and relative salinity, the drops entrain a thin air shell upon entering the mixed layer, which pinches off at the rear and entirely envelops the drop as it plunges into the depths. However, if the drops fall from too high, the impact is too severe for the formation; or from too low, the momentum is not sufficient to entrain the shell around the entire drop (these drops sometimes rest on the tank-water interface for some time). Similar constraints apply if the density differences are too great *et cetera*. Nevertheless, robust drop formation occurs for a reasonably wide span of scales and the (largely uncontrolled) "cleaning" experiment has produced many bubbles. At any one time and in one experiment, the bubbles are alike; but overall, bubbles of diameters from several millimetres to one centimetre occur at *different* times and in *different* experiments.

Here we shall not dwell on the formation process but have more modest aims of suggesting and providing evidence for certain mechanisms and important properties of these bubbles, particularly when they appear to be at rest at some depth below the mixed layer. We also give some (very) limited measurements which provide key dimensions and parameters for these bubbles, at least for one particular day that they occurred.

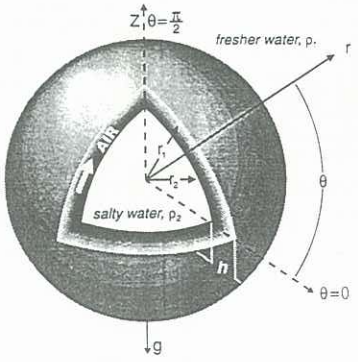

FIGURE 1. Schematic of the thin-film bubbles. Interface radii r_1 and r_2 ($< r_1$), film thickness h and vertical coordinate, z, which is the direction of gravity forces, are shown. The coordinate system origin is at the centre of the approximately concentric spherical interfaces.

Figure 1 shows a schematic of a bubble, with a coordinate system and some parameters defined. By observation these bubbles are spherical, at least to some high degree of approximation. Good estimates are given below of the shape and air-shell thickness, which is inevitably very thin for any moderately stable bubble. The net buoyancy is a combination of the upward force due to the air shell and the excess weight of the inner drop, which is denser than the local ambient fluid. At "equilibrium" this is expressed by

$$(\rho_1 - \rho_{air})r_1^3 = (\rho_2 - \rho_{air})r_2^3 \qquad (1)$$

where the ambient fluid density varies as $\rho(z) = \rho_1 + \rho' z$ and the density of the inner drop is ρ_2. In practice, the approximation $\rho_1 r_1^3 = \rho_2 r_2^3$ determines equilibrium (note that ρ is a single-valued function of depth). Supposing that $\rho_2 = \rho_1(1+\varepsilon)$, then $r_1 = r_2(1 + \frac{1}{3}\varepsilon)$ for small ε. The (initial) mean air-film thickness, h, can be written $h = \frac{1}{3}\varepsilon r_2$. We consider models for the evolution of $h(\theta, t)$ below.

SOME BUBBLE PARAMETERS

Next we list some measurements for a typical set of bubbles generated on one particular day. The impinging drops falling from the membrane had density $\rho_2 = 1.076gcm^{-3}$. The surface tensions of the interfaces involved in bubble formation are unknown, but must be somewhat reduced from that of pure water. The drops fell through a gap of $1.9cm$ into a mixed layer whose density was $\rho = 1.0374gcm^{-3}$. The drops and consequently the bubbles that formed were estimated to be between 3.5 and $4.5mm$ in diameter. These bubbles fell through the mixed

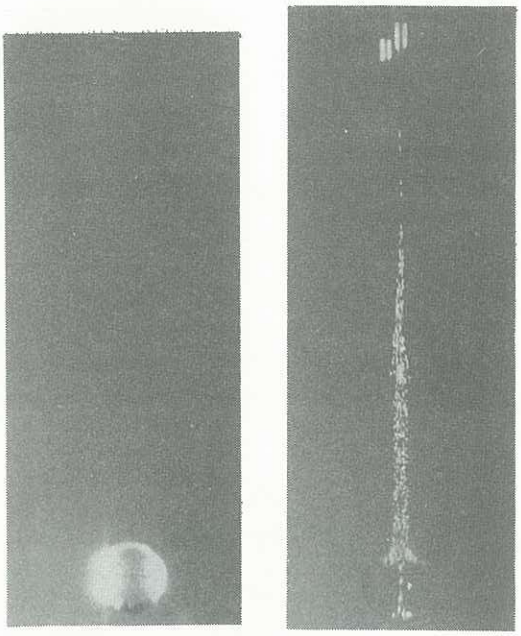

FIGURE 2. Photographs at two instants pre- and post-film rupture. The structure suggested by the pre-rupture contrasting shades is mainly illusory. The air film breaks down into three bubbles and a mist of very small ones.

layer and then through the stratified layer to an average depth of $64cm$, with local density $\rho_1 = 1.0675gcm^{-3}$. This suggests that $h \approx 6\mu m$, i.e. only 0.3% of the bubble radius. Another estimate for h is obtained below. Typically, the bubbles persist at this depth without any change visible to the naked eye for about a minute, then the thin film ruptures, almost in an instant, and a series of small air bubbles are shed. Figure two shows photographs taken at two instants: one prior to rupture and one after. A characteristic to note is that three major air bubbles are shed during rupture but many tiny bubbles are also created. That three major bubbles were shed was a common phenomenon. The time taken for the three major bubbles to rise through the mixed layer (of depth $36cm$) was timed for five different rupture events and the results are shown in table I.

TABLE I. Rise times (seconds)

Largest bubble	:	3.6	4.4	4.85	4.23	4.5
Medium bubble	:	4.9	5.5	6.04	5.79	5.66
Smallest bubble	:	13	12.2	11.76	11.1	12.04

The mean rise velocity of the air bubbles is therefore 8.6, 6.7 and 3.2 cms^{-1} for the largest, medium and smallest bubbles respectively. This velocity is related to the drag on the bubble and its buoyancy. The Reynolds number is of the order of a hundred for the largest bubble, but is smaller for the other two.

Let the bubble rise velocity be U, which we know. The volume of the bubble, and therefore the radius, r, is unknown. The drag coefficient for the bubbles, C_D, is a function of Reynolds number, $Re = 2rU/\nu$, where ν is the kinematic viscosity of the salty water, and of interfacial properties. Two simple, but extreme cases, are considered below. The bubble accelerates in the stratified layer, so that it may be assumed that it rises with terminal velocity for most of the mixed layer; the drag on the bubble then balances the buoyancy, thus

$$\frac{1}{2}\rho\pi r^2 U^2 C_D(Re) = \frac{4}{3}\pi(\rho - \rho_{air})r^3 g \ .$$

Here g is acceleration due to gravity, $g = 980cms^{-2}$. Thus the bubble size is determined by solving

$$\frac{C_D(Re)}{Re} = \frac{4}{3}\frac{g\nu}{U^3} \qquad (2)$$

for Re. Clift *et al.* (1978) give a rough parameterisation of $C_D(Re)$ which is suitable for our needs: $C_D(Re) \approx 14.9Re^{-0.78}$, which assumes negligible surfactant effects (stress free interface). These could well be substantial, in which case treating the bubble as a rigid sphere, with negligible internal air motions, is better (Levich, 1962): the approximation $C_D(Re) \approx \frac{24}{Re}(1 + 0.197Re^{0.63})$ is then useful (from the same source as above).

For the former, we find the shed air bubbles have radii $0.023, 0.019$ and $0.012cm$ for the large, medium and small bubbles respectively and assuming that the "mist" of tiny bubbles have negligible volume, the air film thickness is estimated as approximately $2\mu m$.

Alternatively, but similarly, the rigid-sphere assumption gives the sequence of bubble radii 0.038, 0.030 and $0.016cm$, and consequently an estimate of film thickness of $7\mu m$.

The truth is somewhere in between these two limits (figure 2 roughly supports the latter). This suggests that surfactants do indeed play a role and we must bear this in mind when we consider the drainage of the thin film.

FILM DRAINAGE

Although the bubble remains fixed at the equilibrium depth with no apparent internal or bulk motion, there is necessarily an azimuthal hydrostatic pressure gradient within the air film which must drive the air towards the top of the bubble. It is the remarkable thinness of the air layer, however, which both retards this motion and makes it impossible to discern with the naked eye. To consider the longevity of the bubble we must understand this flow.

Suppose we consider the pressure fields to be everywhere hydrostatic, firstly because the motions are weak, and secondly because the interfaces are very nearly spherical; furthermore, because the bubbles are quite small we locally neglect the gradient of density in the stratified salt water, thus we write

$$p_1 = P_1 - \rho_1 g z$$

as the pressure in the water outside both air-water interfaces, and

$$p_2 = P_2 - \rho_2 g z$$

as the pressure inside both interfaces (P_1 and P_2 are constants). However, this model leads to different tangential pressure gradients either side of the thin air layer for spherical interfaces, which is unacceptable. Suppose instead that we allow the interfaces to deform slightly to equalize this pressure gradient ($\rho_2 - \rho_1$ is small so no gross distortions are required); thus we assign surface tensions σ_2 and σ_1 to the inner and outer *air-water* interfaces respectively. The *air* pressure just inside the outer interface, with curvature κ_1, is p_-, while the air pressure just outside the inner interface, of curvature κ_2, is p_+ and these pressures are given by

$$p_- = P_1 - \rho_1 g z - \sigma_1\kappa_1 \ , \ p_+ = P_2 - \rho_2 g z - \sigma_2\kappa_2 \ .$$

Now, for very thin air films with small $h(\theta, t)$, $\kappa_2 = -\kappa_1$; furthermore, for distortions where $r_1 + R(\theta)$ is the effective shape (of both interfaces) and where $R(\theta)$ is small,

$$\kappa_1 = -\frac{1}{r_1} + \frac{1}{2}\left(R''(\theta) - \tan\theta R'(\theta) + 2R(\theta)\right) \ .$$

The shape is determined by equating the pressure difference across the air film; then the governing linearised equation is

$$R'' - \tan\theta R' + 2R = 2\beta r_1 + 2\frac{\rho_2 - \rho_1}{\sigma_2 + \sigma_1} g r_1^2 z(\theta) \ , \qquad (3)$$

with $z(\theta) = r_1 \sin\theta$. A small residual constant pressure

$$P = P_1 - P_2 + \frac{\sigma_1 + \sigma_2}{r_1} \quad \left(= -\frac{\sigma_1 + \sigma_2}{2r_1}\beta \right)$$

allows the inner drop mass to be fixed for appropriate β. Weak deformations according to (3) require smallness of the parameter

$$2\frac{\rho_2 - \rho_1}{\sigma_1 + \sigma_2} g r_1^2 \quad (= \delta) \ ,$$

which is amply satisfied ($\delta \approx 0.01$) in the present circumstances for $\sigma_1 + \sigma_2 \approx 60$ *dynes/cm*, corresponding to moderately contaminated interfaces (a 0.01% detergent solution has surface tension 30 *dynes/cm*). The resulting shape is

$$R(\theta) = r_1\beta - r_1\frac{1}{3}\delta\,(1 + \sin\theta \log(1 - \sin\theta)) + \tilde{\delta}\sin\theta$$

where $\beta = \frac{1}{3}\delta$ is determined so that volume of the inner drop is preserved. The shape has a degree of arbitrariness since $\tilde{\delta}$ is an unknown constant (but is small), and a logarithmic singularity is predicted at the apex ($\theta = \frac{\pi}{2}$). Other local processes must intervene at the apex; for instance, it is shown below that the film becomes very much thicker at the top ($h \gg h_0$); thus only a more detailed local model can resolve the precise shape. However, a logarithmic singularity is sufficiently mild that no great local distortion is expected; neither is it observed.

Independently of the bubble shape and apex singularity, the pressure gradient in the thin air layer is

$$\frac{1}{r_1}\frac{\partial p}{\partial \theta} = -\left(\frac{\rho_2\sigma_1 + \rho_1\sigma_2}{\sigma_1 + \sigma_2}\right) g\cos\theta \quad (\approx -\rho g\cos\theta) \qquad (4)$$

which is independent of film thickness, i.e. remains constant and always negative for the evolution of the film.

Lubrication theory may be used to consider the film flow (Batchelor, 1967; Borgas & Grotberg, 1988). If we let $r = r_1 - \eta$ define (radial) cross-film distance, so that $0 < \eta < h(\theta, t)$ is the approximate radial extent of the film ($-\frac{\pi}{2} < \theta < \frac{\pi}{2}$ is the azimuthal extent), the velocity profile across the film is

$$u(\eta, \theta, t) = \frac{1}{2}\frac{1}{r_1}\frac{\partial p}{\partial \theta}\frac{1}{\mu_{air}}\eta(\eta - h(\theta, t)) \ . \qquad (5)$$

Here we have assumed that the velocity falls to zero on both interfaces. The resulting shear stress on the interface can be accounted for by azimuthal variation of interfacial surfactant concentration and associated surface tension variation. The surface-tension variation and shear stresses are both weak however, at most of $O(h)$, so that the interfacial effects need not be too strong in any case. Even more complex interfacial rheology is possible in principle (Adamson, 1967), but which usually retard interfacial motions, in support of (5).

Unfortunately, we have few useful facts about the interfacial behaviour for the present system, and choose (5) mainly for simplicity. However, simple stress-free interfaces are considered later (in brief) and are shown to poorly represent the scales of motion, again suggesting an important role for surfactants.

Mass conservation determines the evolution of $h(\theta, t)$ according to the choice of velocity profile. For arbitrary θ, the tangential flux of air integrated around the horizontal azimuth is just

$$Q = 2\pi\cos\theta \int_0^h u(\eta, \theta, t)d\eta \ .$$

This flux prescribes the local rate of change of film thickness (similarly integrated), so that

$$2\pi\cos\theta\frac{\partial h}{\partial t} + \frac{1}{r_1}\frac{\partial Q}{\partial \theta} = 0 \ . \qquad (6)$$

In the case of zero interfacial mass flux (profile (5)), the evolution equation is

$$H_\tau = \sin\theta H^3 - \frac{1}{2}\cos\theta\frac{\partial}{\partial\theta}H^3 \qquad (7)$$

where $h = h_0 H(\theta, \tau)$ and a non-dimensional time scale is used, which is based on uniform initial thickness h_0, such that

$$\tau = t/T \quad \text{where} \quad T = 6\frac{r_1\mu_{air}}{g h_0^2}\left(\frac{\sigma_1 + \sigma_2}{\rho_2\sigma_1 + \rho_1\sigma_2}\right) \ .$$

A unit of τ time corresponds to real time of approximately 0.6 seconds ($= T$).

Two immediate consequences of (7) are that the bottom of the thin layer thins, while the top thickens: in fact

$$H\left(-\frac{\pi}{2}\right) = (1 + 2\tau)^{-\frac{1}{2}} \quad \text{and} \quad H\left(\frac{\pi}{2}\right) = (1 - 2\tau)^{-\frac{1}{2}} \ .$$

The solution appears to be invalid beyond $\tau = \frac{1}{2}$, which suggests that these bubbles are short lived. However, the observations indicate that bubbles exist for times of order a minute ($\tau \approx 100$). The explanation is that the singular behaviour is relatively passive; it heralds the local importance of capillary forces as the curvature increases. It must be remembered that $H \sim 400$ to make the film thickness comparable with bubble size; also that capillary forces are comparable to the hydrostatic pressure forces for radii of curvature $\sim$ 1-2*mm*, and will always keep the peak bounded and smooth. Away from the peak ($\theta \neq \frac{\pi}{2}$) we can find a draining solution of (7) valid for all time.

The draining solution follows most readily from characteristics. We put $\Phi = h^2$, then (7) is equivalent to two coupled ordinary differential equations:

$$\dot{\theta} = \frac{3}{2}\cos\theta\Phi \quad , \quad \dot{\Phi} = 2\sin\theta\Phi^2 \ .$$

The solution then follows as

$$\Phi(\theta(t), t) = \left(\frac{\cos\phi}{\cos\theta}\right)^{\frac{4}{3}}$$

where

$$\frac{3}{2}t\cos^{\frac{4}{3}}\phi = \int_\phi^\theta \cos^{\frac{1}{3}}\theta' d\theta' \quad (\theta > \phi) \qquad (8)$$

with the initial condition $\theta(0) = \phi$. For times smaller than $t = \frac{1}{2}$, ϕ spans the range $-\frac{\pi}{2} < \phi < \frac{\pi}{2}$, but at later times only those ϕ such that $\phi < \varphi$, where

$$\frac{3}{2}t\cos^{\frac{4}{3}}\varphi = \int_\varphi^{\frac{\pi}{2}} \cos^{\frac{1}{3}}\theta' d\theta' \ ,$$

are relevant. The "lost" ϕ values effectively disappear into the singularity at the apex and there is a flux of mass from the film into the singularity. Figure 3a shows the evolution at a series of discrete times for which the film thickness is regular and bounded ($\tau < \frac{1}{2}$). The developing singularity is clearly evident. Figure 3b shows the continuation of the film flow with a singularity, which, after a time reaches a local state described by $\Phi \propto cos^{-\frac{4}{3}}\theta \quad (\theta \approx \frac{\pi}{2})$, with the constant of proportionality a function of time. Overall, however, the film thins, most rapidly, but only algebraically, at the bottom.

The large-time ($\tau \gg 1$) asymptotic solution is useful. In this case only a small band of ϕ values near to $-\frac{\pi}{2}$ remain to contribute. The solution is represented by

$$\mathcal{G}(\theta) = \int_{-\frac{\pi}{2}}^\theta cos^{\frac{1}{3}}\theta' d\theta' \quad \text{with} \quad \Phi = \frac{2}{3}\tau^{-1}\mathcal{G}(\theta)\cos^{-\frac{4}{3}}\theta \quad (9)$$

which is also shown on figure 3b. It is reasonably good for

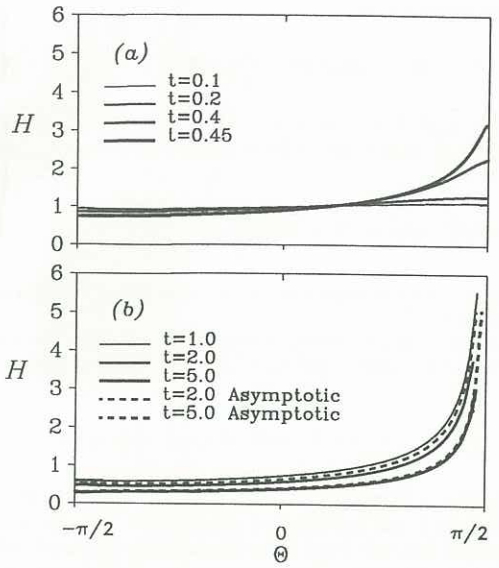

FIGURE 3. Dimensionless bubble thickness H versus azimuthal coordinate θ. *(a)* Regular bubble-film evolution ($\tau < \frac{1}{2}$); *(b)* Bubble-film evolution with an apex singularity. A large-time asymptotic solution is shown for $\tau = 2$ and 5.

times not much larger than $\tau \approx 2$. The volume of air that remains as a *thin* film for large times (i.e., air not "lost" to the growing bubble at the apex) is given by

$$v = \frac{4}{3}\pi r_1^2 h_0 \mathcal{G}^{\frac{3}{2}}\left(\frac{\pi}{2}\right)\sqrt{\frac{2}{3\tau}} \ . \qquad (10)$$

At time $\tau = 100$, and with $\mathcal{G}\left(\frac{\pi}{2}\right) = 2.5871\ldots$, it follows that only about 10% of the initial air-film remains as a redistributed thin film, with the rest accumulating at the apex.

Also at this time the film has thinned to $0.42\mu m$ at the bottom, but is thicker elsewhere. Film rupture seems quite likely at this scale and smaller, although we cannot decide such detail with this simple draining model. It is appealing to imagine that the apex bubble "peels off" owing to its own buoyancy, perhaps splitting into two under capillary forces, while the remaining film almost instantly collapses to a third bubble perhaps at the bottom (the volume fraction of the smallest shed-air-bubble described above is about 10%). However, this is just speculation.

STRESS-FREE INTERFACES

If the surfactants play no significant role, then (5) may only be considered as an initial profile. Water motion must also be generated on both sides of the air film to balance the shear stress on the interfaces. The pressure gradients in the water are virtually hydrostatic, thus water inertia balances the (radial) viscous diffusion of azimuthal momentum during the evolution of the water flows. The variation normal to the interface ($r = r_1 + y$) is more significant than azimuthal variation (but θ is retained as a parameter), thus the simple equation

$$\rho_1 u_t = \mu_1 u_{yy} \ , \qquad (11)$$

where μ_1 is the viscosity of water, determines the evolution of the azimuthal velocity. The initial condition for (11) is $u(y,0) = 0$, and boundary conditions are that far from the interface, $u(\infty,t) = 0$, while on the interface $y = 0$, the tangential stress balance is

$$\frac{\partial u}{\partial y} = \frac{1}{2}\frac{1}{r_1}\frac{\partial p}{\partial \theta}\frac{h(\theta,t)}{\mu_1} \ . \qquad (12)$$

The interface is at rest initially, but from that instant on, the shear-stress imposed by the air accelerates the water and a point on the interface moves upward. It is relatively easy to solve for the motion of the interface using Laplace transforms. Thus

$$u(0,\theta,t) = -\frac{1}{2}\frac{1}{r_1}\frac{\partial p}{\partial \theta}\frac{\sqrt{\nu}}{\sqrt{\pi}\mu_1}\int_0^t \frac{h(\theta,t-t')}{\sqrt{t'}}dt' \ , \qquad (13)$$

where ν is the kinematic viscosity of water. The interfacial velocity is the same on both sides of the air-film; in fact the two velocity fields, (5), and a "plug" flow with velocity (13), are just superimposed in the air film. This modifies the air-film thickness evolution equation, making it quite complicated. However, as before, the evolution of the bottom of the film ($\theta = -\frac{\pi}{2}$) is simpler:

$$H_\tau = -\lambda H(\tau)\int_0^\tau \frac{H(\tau-\tau')}{\sqrt{\tau'}}d\tau' - H^3(\tau) \qquad (14)$$

where $\lambda = \frac{6}{\sqrt{\pi}}\frac{\sqrt{\nu T}}{h_0}\frac{\mu_{air}}{\mu_1} \approx 4.3$. The large time ($\tau \gg 1$) approximation

$$H_\tau = -\frac{\lambda}{\sqrt{\tau}}H(\tau)\int_0^\infty H(\tau')d\tau'$$

suggests that $H \propto e^{-\alpha\sqrt{\tau}}$ for some constant α. If this large time solution is approximately valid for all time (putting $H(0) = 1$), then $\alpha^3 \approx 4\lambda$ so that $\alpha \approx 2.6$. In fact a numerical solution gives $\alpha = 0.78\lambda = 3.35$.

Therefore the film thins *exponentially* fast, and, in time $\tau = 10$ (6 seconds of real time), the film has thinned to less than $2\mathring{A}$ at the bottom, and is not much longer for this world. Thus neglecting the influence of surfactants clearly leads to more rapid draining than is possible according to the observed bubble lifetimes (~ 60 seconds).

DISCUSSION

The properties of the observed bubbles seem readily explicable with standard fluid mechanical models, although none of the models used can be considered entirely accurate or absolutely correct. Uncertainty remains with the specification of interfacial properties. In particular, the role of surfactants is crucial. Nevertheless, the scales of the motions and bubble dimensions are explained quite well with the simple approximations made. If nothing else, this discourse illustrates some of the complexities of contaminated interfacial mechanics, and perhaps some of the fascination.

ACKNOWLEGEMENTS

George Scott and David Whillas provided valuable assistance with the experiments and photographs used in this paper.

REFERENCES

ADAMSON, A W (1967) Physical Chemistry of Surfaces. Interscience (2nd Edition).

BATCHELOR, G K (1967) An Introduction to Fluid Dynamics. Cambridge University Press.

BORGAS, M S & GROTBERG, J B (1988) Monolayer flow on a thin film. J. Fluid Mech., 193, 151-170.

BOYS, C V (1890) Soap Bubbles and the Forces that Mould Them. Society for Promoting Christian Knowledge, London.

CLIFT, R, GRACE, J R & WEBER M E (1978) Bubbles, Drops and Particles. Academic Press.

HIBBERD, M F & SAWFORD, B L (1989) A Laboratory model of convection in the atmospheric boundary layer. Proc 10th Australasian Fluid Mech Conf, Melbourne, II, 14.17-14.20.

LEVICH, V G (1962) Physicochemical Hydrodynamics. Prentice-Hall.